Stem Cell Research (2009) 3, 126–141

available at www.sciencedirect.com

ScienceDirect

www.elsevier.com/locate/scr

REGULAR ARTICLE

BMP inhibition stimulates WNT-dependent generation of chondrogenic mesoderm from embryonic stem cells

Makoto Tanaka [a,b,1], Vanta Jokubaitis [b,2], Colin Wood [a], Yi Wang [a,b], Nathalie Brouard [a,3], Martin Pera [b,4], Milton Hearn [d], Paul Simmons [a,3], Naoki Nakayama [a,b,c,*,3]

[a] *Peter MacCallum Cancer Institute, East Melbourne VIC 3002, Australia*
[b] *Australian Stem Cell Centre, Clayton VIC 3800, Australia*
[c] *Department of Anatomy and Developmental Biology, Monash University, Clayton VIC 3800, Australia*
[d] *Centre for Green Chemistry, Monash University, Clayton VIC 3800, Australia*

Received 12 February 2009; received in revised form 22 June 2009; accepted 10 July 2009

Abstract WNT and bone morphogenetic protein (BMP) signaling are known to stimulate hemogenesis from pluripotent embryonic stem (ES) cells. However, osteochondrogenic mesoderm was generated effectively when BMP signaling is kept to a low level, while WNT signaling was strongly activated. When mesoderm specification from ES cells was exogenous factor dependent, WNT3a addition supported the generation of cardiomyogenic cells expressing lateral plate/extraembryonic mesoderm genes, and this process involved endogenous BMP activities. Exogenous BMP4 showed a similar effect that depended on endogenous WNT activities. However, neither factor induced robust chondrogenic activity. In support, ES cell differentiation in the presence of either WNT3a or BMP4 was associated with elevated levels of both Bmp and Wnt mRNAs, which appeared to provide sufficient levels of active BMPs and WNTs to promote the nonchondrogenic mesoderm specification. The osteochondrogenic mesoderm expressed PDGFRα, which also expressed genes that mark somite and rostral presomitic mesoderm. A strong WNT signaling was required for generating the mesodermal progeny, while approximately 50- to 100-fold lower concentration of WNT3a was sufficient for specifying axial mes(end)oderm. Thus, depending on the dose and cofactor (BMP), WNT signaling stimulates the generation of different biological activities and specification of different types of mesodermal progeny from ES cells.

* Corresponding author. Centre for Stem Cell Research, Brown Foundation Institute of Molecular Medicine, The University of Texas Health Science Center at Houston, SRB 637C, 1825 Pressler St., Houston, TX 77030, USA. Fax: +1 713 500 2424.
E-mail address: naoki.nakayama@uth.tmc.edu (N. Nakayama).
[1] Current address: Department of Orthopaedic Surgery, Graduate School of Medicine, Osaka University, Suita, Osaka, Japan.
[2] Current address: Monash Immunology and Stem Cell Laboratories, Monash University, Clayton VIC 3800, Australia.
[3] Current address: Center for Stem Cell Research, Institute of Molecular Medicine, University of Texas Health Science Center, Houston, TX 77030.
[4] Current address: Center for Regenerative Medicine and Stem Cell Research, University of Southern California School of Medicine, Los Angeles, CA 90033.

1873-5061/$ – see front matter © 2009 Elsevier B.V. All rights reserved.
doi:10.1016/j.scr.2009.07.001

Introduction

Chondrogenesis occurs primarily during embryogenesis. Chondrocyte precursors arise from particular mesoderm and the neural crest. For example, sclerotome, responsible for the genesis of axial skeleton, is derived from somite, epithelialized paraxial mesoderm that marks a distromedial region of the mouse embryo. The limb bud mesenchyme responsible for appendicular skeletogenesis is derived from somatopleura, a dorsal part of lateral plate mesoderm that marks the proximolateral region of the mouse embryo. Pluripotent embryonic stem (ES) cells have been shown to give rise to many mesodermal derivatives, such as cartilage, bone, muscle, and blood cells (Doetschman et al., 1985; Robertson, 1987). We have previously demonstrated that ES cell progeny form hyaline cartilage particles when isolated and pellet-cultured in the presence of both platelet-derived growth factor (PDGF) and transforming growth factor-β (TGFβ), with the subsequent removal of TGFβ (Nakayama et al., 2003). In particular, progeny expressing the PDGF receptor alpha chain (PDGFRα), but not the vascular endothelial growth factor (VEGF) receptor-2 (FLK1), i.e., $FLK1^{-}PDGFR\alpha^{+}$ ($F^{-}P^{+}$) cells, generate cartilage nodules even when TGFβ is absent at all times.

In vitro differentiation seems to follow early embryogenic events (Keller, 2005; Nishikawa et al., 2007). Generation of a particular mesodermal progeny from ES cells is therefore determined by the expression of embryonic stage-, location-, and lineage-restricted cell surface markers and genes, and the representative biological activities. ES cells readily give rise to progeny expressing N-cadherin (CDH2) (Honda et al., 2006), PDGFRα, and/or FLK1 (Nakayama et al., 2003; Nishikawa et al., 1998a). Early in mouse embryogenesis, Cdh2 is widely expressed in mesoderm (Radice et al., 1997), and Flk1, which is essential for embryonic hematopoiesis and vasculogenesis, is expressed in proximolateral/extraembryonic mesoderm (Takakura et al., 1997). Pdgfra is essential for the normal development of many mesodermal tissues, including the axial skeleton (Betsholtz et al., 2001), and is expressed strongly in paraxial mesoderm (Takakura et al., 1997). Consistently, F^{+} and P^{+} progeny contain cells specified to lateral plate mesoderm and paraxial mesoderm, respectively (Nishikawa et al., 1998a; Sakurai et al., 2006). Therefore, the TGFβ-independent chondrogenic activity found in the $F^{-}P^{+}$ cell fraction may be characteristic of somitic mesoderm and/or sclerotome. However, our preliminary transcriptome analysis indicated that the chondrogenic $F^{-}P^{+}$ cells express characteristics of lateral plate and/or extraembryonic mesoderm, but not somitic mesoderm. To investigate the basis of the chondrogenic activity we have sought ways of directing ES cells to differentiate into particular types of mesodermal progeny.

The formation of mesodermal progenitors from primitive ectoderm (epiblast) and the later restriction of their developmental potentials are tightly regulated in vivo by the activities of several growth and differentiation factors such as Wnt proteins and members of the TGFβ superfamily: TGFβ, Activin, Nodal, and bone morphogenetic protein (BMP). To establish conditions that lead to preferential generation of particular mesodermal progeny, previous studies have examined the roles of these factors on ES cell differentiation (Nakayama et al., 2000, 2003; Lengerke et al., 2008; Nostro et al., 2008). The early mesoderm marker gene, Brachyury (T), essential for somite formation (Rashbass et al., 1991), is induced in response to BMP4 under serum-free conditions (Johansson and Wiles, 1995; Wiles and Johansson, 1999; Fehling et al., 2003) in accord with the crucial role of BMP4 and its receptor BMPR1A in gastrulation and subsequent mesoderm formation in vivo (Mishina et al., 1995; Winnier et al., 1995). BMP4 is essential for the generation of blood cells (Nakayama et al., 2000) and allows the formation of bone and cartilage progenitors (Nakayama et al., 2003) from ES cells. Wnt proteins are also involved in mesoderm formation (Houston and Wylie, 2004). For example, T expression is controlled by Wnts (Yamaguchi et al., 1999; Arnold et al., 2000), Wnt3 is essential for the onset of gastrulation, needed for mesoderm formation (Liu et al., 1999), and Wnt3a regulates the fate of dorsal mesoderm and is required later for the generation of all new embryonic mesoderm (Takada et al., 1994; Yoshikawa et al., 1997). Consistently, canonical WNT signaling is essential for hemogenesis from ES cells, which is upregulated by overexpression of Wnt3 (Lindsley et al., 2006; Lako et al., 2001).

Here, we address how WNTs and BMPs control the generation from ES cells of osteochondrogenic mesodermal progeny expressing characteristics of somitic mesoderm. We demonstrate that specification of lateral plate/extraembryonic mesoderm and paraxial mesoderm requires stronger WNT signaling than specification of mes(end)oderm, and that involvement of BMP signaling in this process restricts the type of specified mesoderm to lateral/extraembryonic mesoderm. Efficient chondrogenic mesoderm genesis correlates with somitic/rostral presomitic mesoderm specification, which is only achieved when BMP signaling is silenced. We also provide evidence for cross-feedback between the expression of Wnt and Bmp genes, such that addition of either WNTs or BMPs leads to differentiation involving both BMP and WNT signaling. BMP inhibitor therefore plays a critical role in the WNT3a-dependent generation of somitic mesoderm-like chondrogenic cells from ES cells.

Results

Somitic mesoderm is specified by endogenous WNT activity specifically in the presence of low or absent BMP signaling in Knockout Serum Replacement-based serum-free medium

During ES cell differentiation in the presence of BMP4 in a Knockout Serum Replacement (KSR)-based serum-free medium, hemoangiogenic cells are identified by the expression of FLK1 and lack of PDGFRα ($F^{+}P^{-}$), while chondrogenic activity is present in $F^{+}P^{-}$ and $F^{-}P^{+}$, and to a limited degree, in $F^{+}P^{+}$ populations (Nakayama et al., 2003). In the absence of BMP4 or the presence of the BMP inhibitor, Noggin (fused with IgG1-Fc, NOG), the genesis of $F^{+}P^{+}$ and $F^{+}P^{-}$ cells was hardly detectable, but $F^{-}P^{+}$ progeny were generated at significant levels (Fig. 1A, -BMP/Fc, ±BMP/NOG). The likely mesodermal origin of these cells has been confirmed by their expression of both T (as shown by flow cytometric analysis of Green fluorescent protein (GFP)-Bry ES cells differentiated under identical conditions; Supplemental Fig. 1A or S. Fig. 1A) and N-cadherin (CDH2 or N) (Fig. 1B), and by the absence of E-cadherin (data not shown).

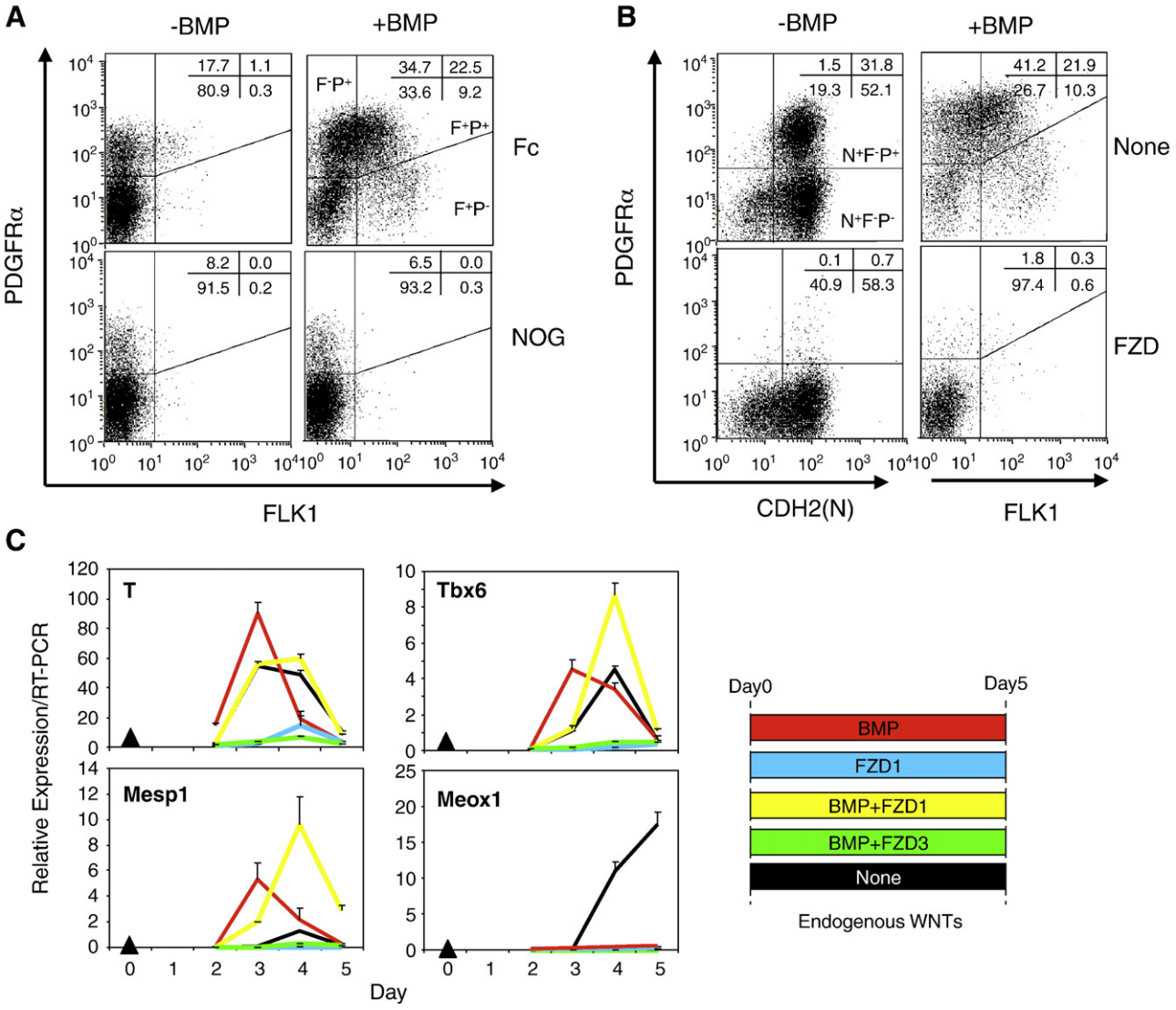

Figure 1 NOG-resistant and FZD-sensitive generation of progeny expressing rostral paraxial mesoderm genes. (A) The E14 ES cells were differentiated for 4.7 days in KSR-medium with (+BMP) or without BMP4 (-BMP) with IgG-Fc (Fc) or NOG (NOG) at 1 μg/ml, and FACS-analyzed for FLK1 and PDGFRα expression. Profiles represent more than 20 independent experiments. (B) ES cells were differentiated as in (A) in the presence of 1 μg/ml (−BMP, FZD), 3 μg/ml (+BMP, FZD), or zero (+/−BMP, None) FZD, and analyzed by FACS for CDH2, FLK1, and PDGFRα expression. (A, B) The numbers in the top right corner of each profile are the percentage total viable cells of the corresponding quadrants. The relevant cell populations are indicated in representative profiles. (C) Effects of FZD on mesodermal gene expression. E14 cells were differentiated with or without BMP4 in the absence or presence of 1 μg/ml (FZD1) or 3 μg/ml (FZD3) FZD. Real-time RT-PCR was performed on EBs with primer sets for T, Tbx6, Mesp1, and Meox1 genes. Right panel: schedule for factor addition (color coded). The line color corresponds to the color code. ▲, Day 0 control. The results are presented as average relative expression levels with standard deviation (SD) shown as thin vertical lines, and are representative of two independent experiments.

Involvement of WNT signaling in the genesis of such F^+ and/or P^+ mesodermal cells was demonstrated by addition of the WNT inhibitors, mouse Frizzled-8 extracellular domain (fused with IgG1-Fc, FZD, Fig. 1B) and Dickkopf1 (DKK1) (data not shown). FZD caused complete suppression at 1 μg/ml in the absence of BMP4 (-BMP/FZD), and at 3 μg/ml in the presence of BMP4 (+BMP/FZD), in accord with previous observations (Lindsley et al., 2006). [Note that F^-P^+ progeny derived from BMP4-untreated or NOG-treated embryoid bodies (EBs) are indicated with N^+ hereafter to distinguish them from progeny derived from BMP4-treated EBs.]

To determine the types of mesodermal progeny generated in the presence or absence of BMP4, the expression of T (Rashbass et al., 1991; Wilkinson et al., 1990), a marker of primitive streak and early mesoderm; Mesp1 (Saga et al., 1996), a marker of posterior primitive streak and early mesoderm; and Mox1/Meox1 (Candia et al., 1992; Mankoo et al., 2003); and Tbx6 (Chapman et al., 1996; Chapman and Papaioannou, 1998), markers of paraxial mesoderm, was investigated by real-time RT-PCR during the first 5 days of differentiation of E14 (Fig. 1C) and Rosa26 (S. Fig. 1C) ES cells. Commonly, expression of T and its target gene Tbx6 was

independent of BMP4 (black, red), Meox1 was induced only in the absence of BMP4 (black) and Mesp1 only in its presence (red). These data therefore suggest that some paraxial mesoderm is preferentially generated in the presence of a very low or absent BMP activity, correlating with the genesis of cells displaying the $N^+F^-P^+$ phenotype (Figs. 1A and B, -BMP/Fc, ±BMP/NOG, -BMP/None). Inhibition of Wnt signaling with FZD at 1 μg/ml in the absence of BMP4 (Fig. 1C, blue) almost completely suppressed the expression of T, Tbx6, and Meox1, while in BMP4-treated cultures, T and Tbx6 expression disappeared only with 3 μg/ml FZD (green). Interestingly, T, Tbx6, and Mesp1 mRNAs appeared approximately 1 day earlier in the presence of BMP4 (red), an effect that was reversed with 1 μg/ml FZD (yellow).

These results indicate that specification of mesoderm during ES cell differentiation in the presence or absence of BMP4 in a KSR-based serum-free medium involves endogenous WNT activity; activation of both WNT and BMP signaling is likely to specify F^+ hemogenic mesoderm and potentially other lateral plate/extraembryonic mesoderm, and activation of WNT but not BMP signaling leads to preferential specification of paraxial mesoderm.

Identification and isolation of somitic mesoderm-like cells using PDGFRα, FLK1, and CDH2 markers

To characterize Meox1-expressing paraxial mesoderm, the $N^-F^-P^-$, $N^+F^-P^-$, and $N^+F^-P^+$ cell populations derived from Day 3.7–4.7 EBs generated in KSR medium without BMP4 were individually isolated by fluorescence-activated cell sorting (FACS) (gates 2, 3 and 4, respectively, Fig. 2A, -BMP), and then subjected to transcriptional profiling analysis. As a control, F^-P^-, F^-P^+, F^+P^+, and F^+P^- cell populations generated with active BMP and WNT signaling were isolated from BMP4-treated EBs as described (Nakayama et al., 2003) (Fig. 2A, +BMP, gates 6, 7, 8, and 9).

Strikingly, transcripts marking somite and the anterior tip of presomitic mesoderm, such as Paraxis/Tcf15 (Burgess et al., 1995, 1996), Uncx4.1 (Mansouri et al., 1997; Neidhardt et al., 1997), Tbx18 (Kraus et al., 2001), and Mesp2 (Saga et al., 1997) and those marking differentiating somite and sclerotome, such as Pax1 (Deutsch et al., 1988) and Meox1, were restricted to the $N^+F^-P^+$ fraction from BMP4-untreated EBs (Fig. 2B, and S. Figs. 2A and 3A, lane 3) and were not detected in fractions derived from BMP4-treated EBs. In contrast, consistent with the results of previous bioassays (Nakayama et al., 2003; Sakurai et al., 2006), transcripts of Hand2 (Srivastava et al., 1997) and Foxf1a (Mahlapuu et al., 2001; Peterson et al., 1997), marker genes for lateral plate and extraembryonic mesoderm, were enriched in the F^-P^+ and F^+P^+ fractions from BMP4-treated EBs (Fig. 2C, lanes 7 and 8). In addition, genes expressed in hemangioblasts and primitive hematopoietic and endothelial cells, which are derivatives of lateral plate/extraembryonic mesoderm, e.g., Scl/Tal1 (Elefanty et al., 1999; Chung et al., 2002), Cdh5 (Breier et al., 1996; Nishikawa et al., 1998a,b), Cd34 (Young et al., 1995; Wood et al., 1997) (Fig. 2C, and S. Figs. 2A and 3B), Ikzf1 (Ikaros), Hhex, Tie2/Tek (Angiopoietin-1 receptor), and Flt1 (VEGF receptor-1) (Supplemental Table 2 or S. Table 2), were present exclusively in the F^+P^- fraction (lane 9) from BMP4-treated EBs.

Collectively, this transcriptional profiling analysis suggests that P^+ progeny (i.e., $N^+F^-P^+$ cells) generated by Days 3.7–4.7 of differentiation with WNT but not BMP signaling are enriched for cells specified to somitic and/or rostral presomitic mesoderm, and F^+ and P^+ progeny generated by a combination of WNT and BMP signaling are enriched for cells specified to lateral plate and/or extraembryonic mesoderm.

In vitro chondrogenic, osteogenic, and myogenic activities of the isolated somitic mesoderm-like cells

To test the hypothesis that the $N^+F^-P^+$ cell fraction is enriched in cells specified to somitic/rostral presomitic mesoderm, these cells were subjected to pellet micromass culture and their capacity to generate chondrocytes determined. The $N^+F^-P^+$ cells formed more cartilage-matrix-containing particles in the presence of TGFβ3 than in its absence (Fig. 3A, left). However, the same cells failed to develop lymphoid or erythro-myeloid progenitors on OP9 cells (data not shown), therein resembling F^-P^+ cells derived from BMP4-treated EBs (Nakayama et al., 2003). Furthermore, comparison of the chondrogenic potential of the $N^-F^-P^-$, $N^+F^-P^-$, and $N^+F^-P^+$ fractions using a two-dimensional (2D)-micromass culture assay revealed that the $N^+F^-P^+$ fraction contained the most chondrocyte precursors as determined by Alcian blue-stained matrix deposition in response to TGFβ3 (Fig. 3A, right). The $N^+F^-P^+$ cells were also able to proliferate in 2DIF medium and, when transferred to the osteoinductive medium (BOM), deposited higher levels of mineral than the $N^+F^-P^-$ cells, suggesting that the $N^+F^-P^+$ EB cells contained or generated osteoblast-like cells (Fig. 3B). During the 2D-micromass culture in the absence of TGFβ3, the $N^+F^-P^+$ population also gave rise to clusters of spindle-shaped skeletomyocyte-like cells, visualized with the skeletal myosin antibody (Fig. 3C), and self-beating cardiomyocyte-like cells, stained with an antibody to cardiac β-myosin (data not shown). These findings suggested that the $N^+F^-P^+$ cell fraction is also enriched for myogenic activity, consistent in part with previous observations (Sakurai et al., 2008; Darabi et al., 2008). Thus, in support of our hypothesis, these data indicate that the $N^+F^-P^+$ cell fraction is enriched in (precursors of) osteochondrogenic and myogenic cells.

Depending on the dose and the presence of BMP-inhibitor exogenous WNT3a specifies different mesoderm in chemically defined medium

To further investigate the role of WNTs on chondrogenic mesoderm specification during ES cell differentiation, we determined the optimal strength of WNT signaling using modified Johansson and Wild's chemically defined medium (CDM), in which mesoderm formation, i.e., T^+ cell genesis, became dependent on exogenous WNT3a.

In contrast to differentiation in the KSR medium, no F^+ progeny and very few P^+ progeny were generated in the first 5–6 days of differentiation in the absence of exogenous factors in CDM (Fig. 4A, None), and the T transcript was barely detectable (Fig. 4B, lane 2). However, lateral plate/extraembryonic mesoderm specification occurred when

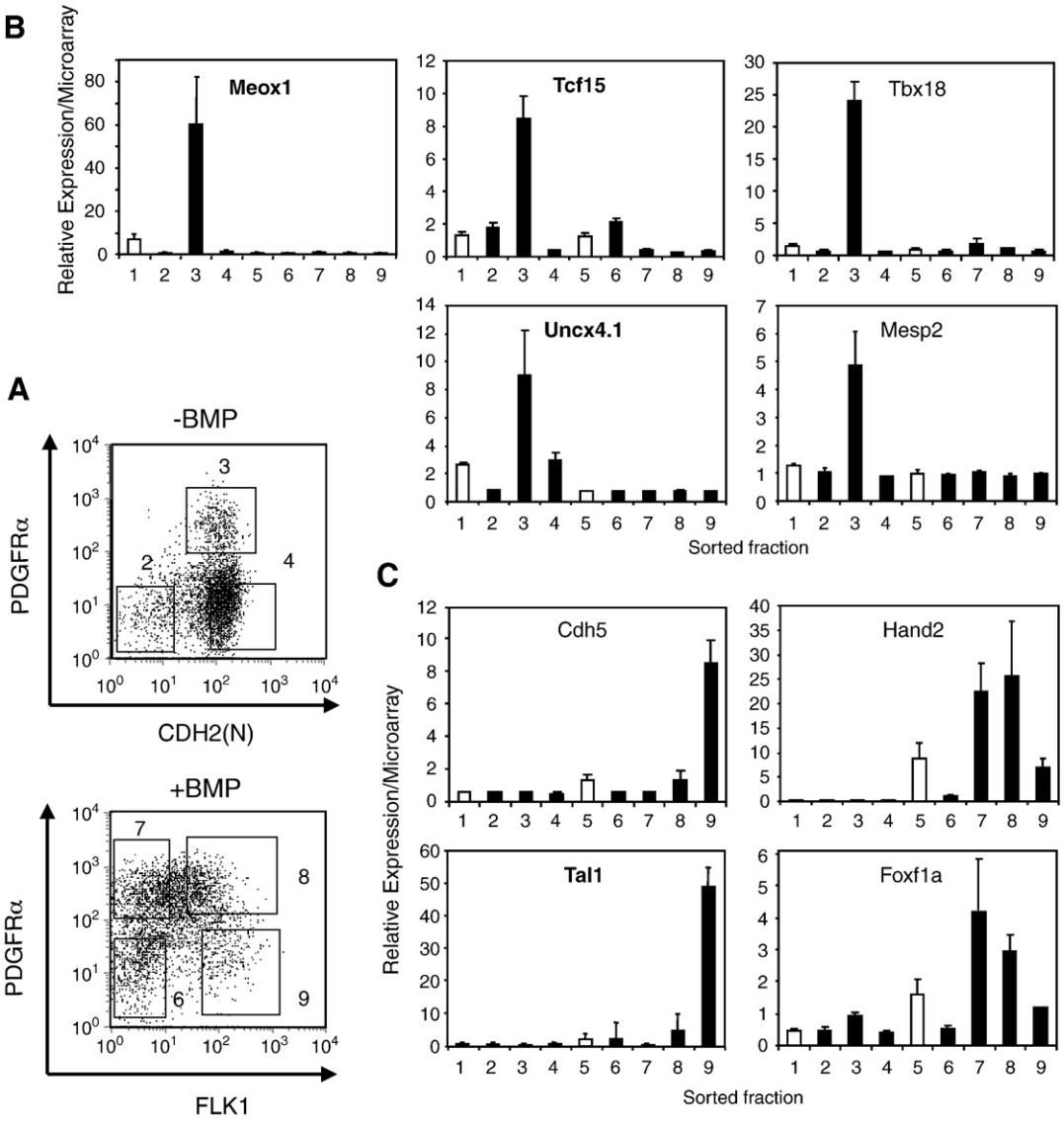

Figure 2 Differential enrichment for somitic/rostral presomitic mesoderm, and lateral plate/extraembryonic mesoderm by FACS. (A upper) Fractionation of EB cells derived from the BMP4-untreated differentiation culture in KSR-based serum-free medium. E14 EB cells were sorted using the gates shown: $N^-F^-P^-$ (gate 2); $N^+F^-P^+$ (gate 3); $N^+F^-P^-$ (gate 4). (A lower) In the presence of BMP4, EB cells were sorted into F^-P^- (gate 6), F^-P^+ (gate 7), F^+P^+ (gate 8), and F^+P^- (gate 9). Profiles are representative of at least 10 independent experiments. (B) Expression of the typical somitic/rostral presomitic mesoderm genes Meox1, Tcf15, Tbx18, Uncx4.1, and Mesp2 in each fraction. (C) Expression of Hand2 and Foxf1a representing lateral plate/extraembryonic mesoderm, and Cdh5 and Tal1 representing their hemoangiogenic derivatives. Real-time RT-PCR showed very similar patterns (gene symbols in bold, S. Fig. 3). Data are the normalized relative expression level for microarray with standard error (SE) shown as thin vertical lines. The sample/lane number matches the gate number, except that 1 and 5 represent unsorted EB cells generated without and with BMP4, respectively (white bars).

WNT3a was added to a concentration of more than 10 ng/ml, as assessed by the appearance of Mesp1, Hand2 (data not shown), and Foxf1a (Fig. 4B, lane 6/W, and Fig. 4C, purple) transcripts. The levels of transcripts reached a plateau at 50 to 100 ng/ml WNT3a. Tal1 expression was also induced (Fig. 4C, purple), suggesting the genesis of hemoangiogenic cells, and the level continued to increase, even at 200 ng/ml (data not shown). In parallel, WNT3a induced the generation of F^-P^+ cells and to a lesser extent F^+P^- cells from ES cells (20–30 and 3–5% of total EB cells, respectively, Fig. 4A, W). However, the expression of somitic/rostral presomitic mesoderm genes such as Meox1 and Uncx4.1 was never detected in the presence of 5–250 ng/ml of WNT3a (Fig. 4B, lane 6/W, and Fig. 4C, purple). In contrast, expression of the marker genes for anterior primitive streak, node, and axial mes(end)oderm, such as Foxa2/Hnf3b(Monaghan et al., 1993; Ang et al., 1993; Sasaki and Hogan, 1993) and Chordin (Chrd) (Bachiller et al., 2000), showed a bell-shaped response to WNT3a in the concentration range 2–10 ng/ml, with the peak at about 5 ng/ml, consistent with the previous

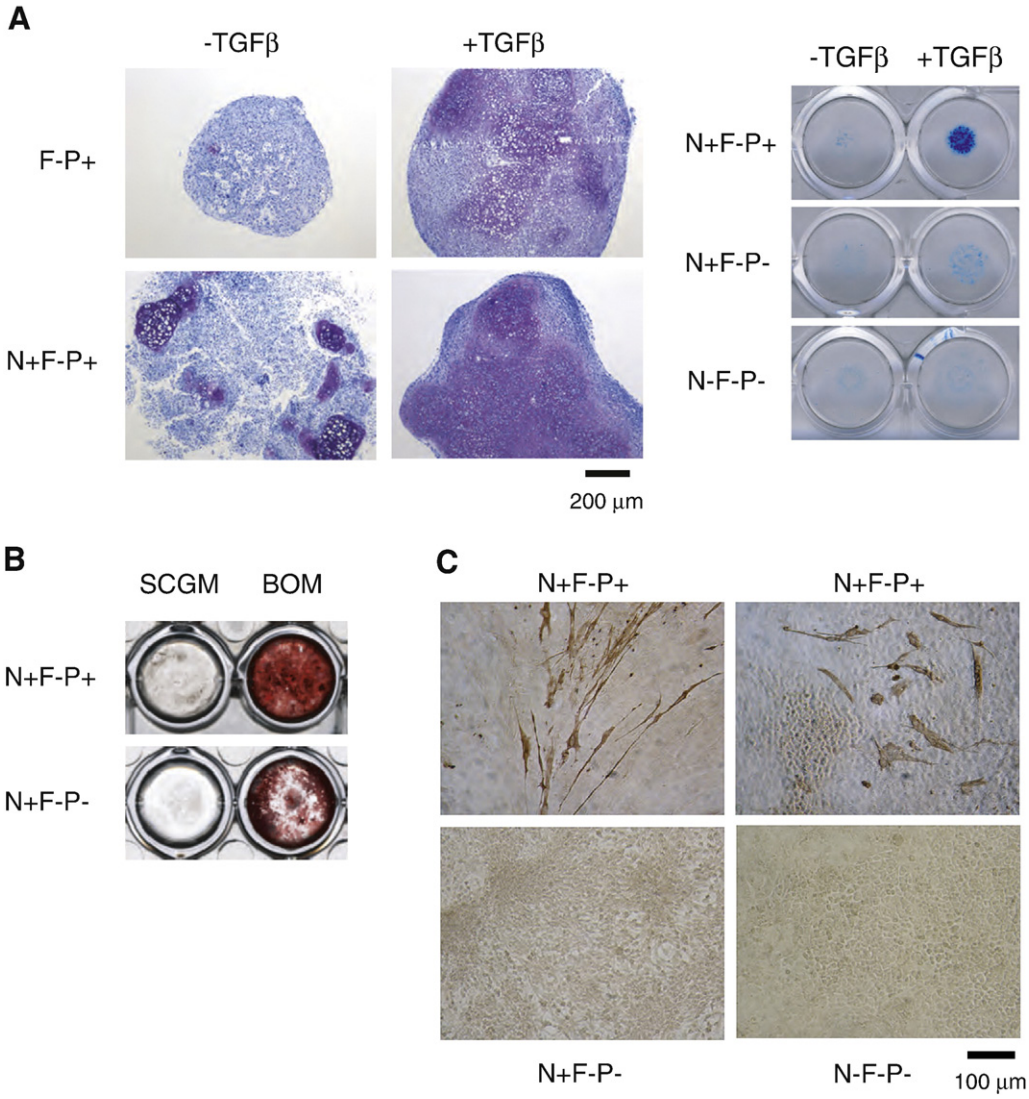

Figure 3 Osteochondrogenic and skeletomyogenic activities of the $N^+F^-P^+$ rostral paraxial mesoderm cells. (A) Chondrogenic property. (Left) Pellet culture: F^-P^+ cells from BMP4-treated E14 EBs (F^-P^+), and those from 0.5 μg/ml NOG-treated EBs ($N^+F^-P^+$) were subjected to serum-free pellet culture in the absence of PDGF with (+TGFβ) or without (-TGFβ) TGFβ3. Particles formed over 15 days of culture were formalin-fixed, paraffin-embedded, sectioned, and stained with toluidine blue. The results are representative of 3 independent experiments. (Right) 2D-Micromass culture: $N^+F^-P^+$, $N^+F^-P^-$, and $N^-F^-P^-$ cells from BMP4-untreated EBs were individually spotted for micromass culture in 2DFCS with (+TGFβ) or without (-TGFβ) TGFβ3. Cultures were fixed on Day 10, and stained with Alcian blue. (B) Osteogenic property. Sorted cells from BMP-untreated E14 EBs were individually expanded in 2DIF for 3–4 days, when mineralization was induced by BOM for 4 weeks. Un-induced controls were cultured in SCGM. Mineral deposition was revealed by staining with Alizarin red. (C) Skeletomyogenic activity. Sorted cells from BMP-untreated E14 EBs were subjected to 2D-micromass culture without TGFβ3, and immunostained with MF20 on Day 10.

observation (Fig. 4C, purple) (Nostro et al., 2008). WNT3a above 10 ng/ml was somewhat inhibitory. Therefore, during the first 5 days of ES cell differentiation, a low concentration of WNT3a preferentially specifies axial mes(end)oderm and a higher concentration promotes lateral plate/extraembryonic mesoderm specification.

Exogenous WNT3a required the presence of BMP-inhibitor NOG to stimulate expression of genes representing somitic/rostral presomitic mesoderm such as Tcf15, Tbx18 (data not shown), Meox1, and Uncx4.1 (Fig. 4B, lane 7/WN, and Fig. 4C, orange) in a dose-dependent manner; however, the lateral plate/extraembryonic mesoderm markers Hand2 (data not shown) and Foxf1a were not detected in the presence of NOG. The dose of WNT3a required was similar to that for lateral plate/extraembryonic mesoderm specification. In the presence of NOG, WNT3a consistently induced the generation of F^-P^+ cells from ES cells (Fig. 5A, WN). However, axial mes(end)oderm marker gene expression lost the bell-shaped response to WNT3a (Fig. 4C, orange). The expression levels reached a plateau at about 5–10 ng/ml WNT3a and did not decrease at concentrations of up to 250 ng/ml, indicating that WNT3a specification of axial mes(end)oderm is actively inhibited by endogenous BMP functions when WNT3a is provided at a high concentration.

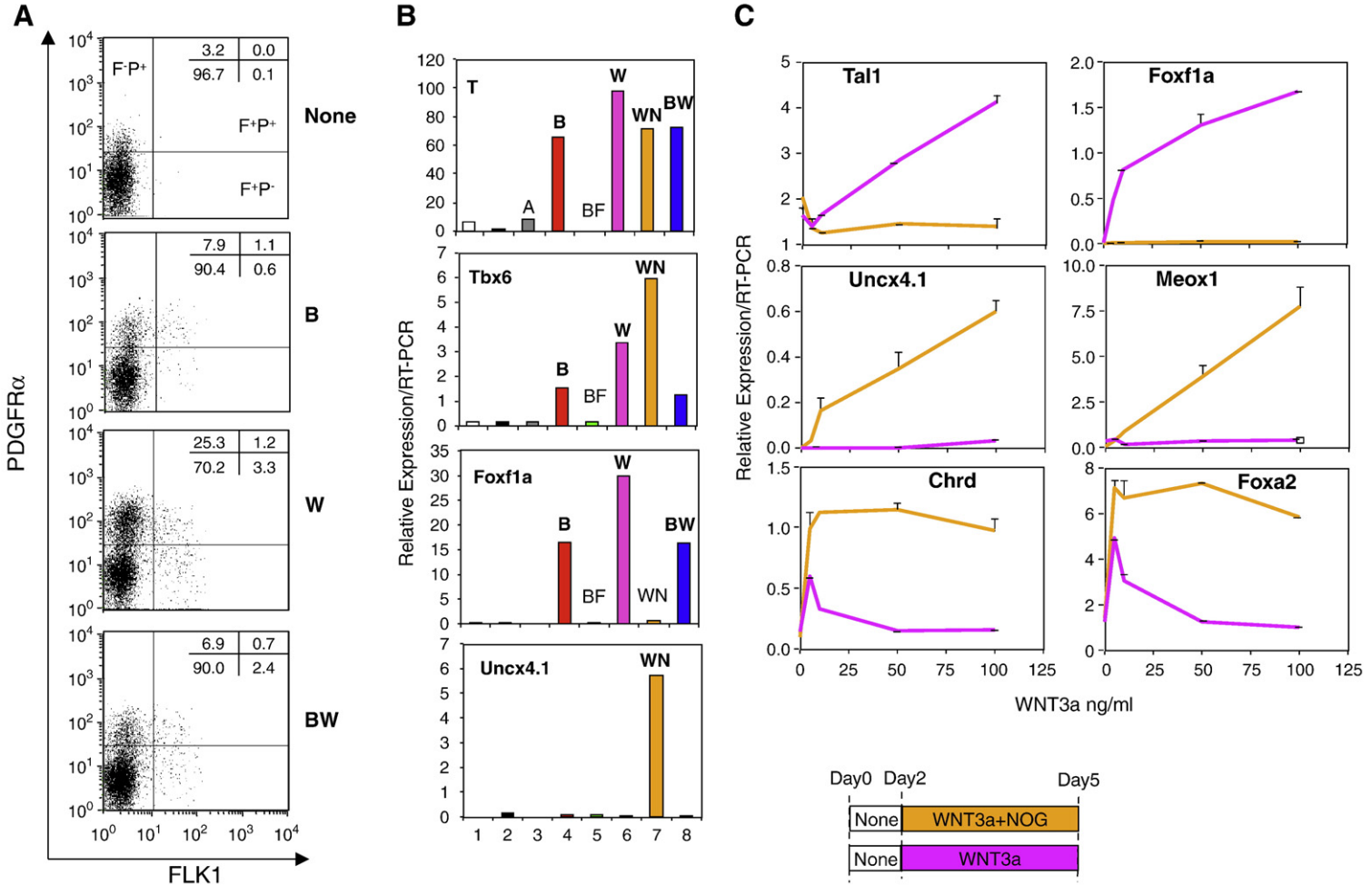

Figure 4 Exogenous WNT3a-induced specification of mesoderm from ES cells is concentration dependent and involves endogenous BMP functions. (A) The E14 ES cells differentiated in CDM in the presence of no factor (None), BMP4 (B), 100 ng/ml WNT3a (W), and BMP4+WNT3a (BW) were FACS-analyzed on Day 5. The numbers in the top right corner of each profile are the percentage total viable cells of the corresponding quadrants. The profiles were representative of 3 independent experiments. (B) E14 cells (lane 1) were differentiated in CDM with no factor (lane 2), 25 ng/ml Activin (A, lane 3), BMP4 (B, lane 4), BMP4+3 μg/ml FZD (BF, lane 5), WNT3a (W, lane 6), WNT3a+0.5 μg/ml NOG (WN, lane 7), and BMP4+WNT3a (BW, lane 8), added on Day 2. (C) E14 cells were differentiated in CDM in the presence of 0 (purple line) or 0.5 μg/ml NOG (orange line) with 0, 5, 10, 50, or 100 ng/ml WNT3a added on Day 2. (B, C) EBs were harvested on Day 5, and extracted RNAs were subjected to real-time RT-PCR using primers for Tal1, Foxf1a, Uncx4.1, Meox1, Chrd, and Foxa2. The results, presented as average relative expression levels with SD shown as thin vertical lines, are representative of 3 independent experiments.

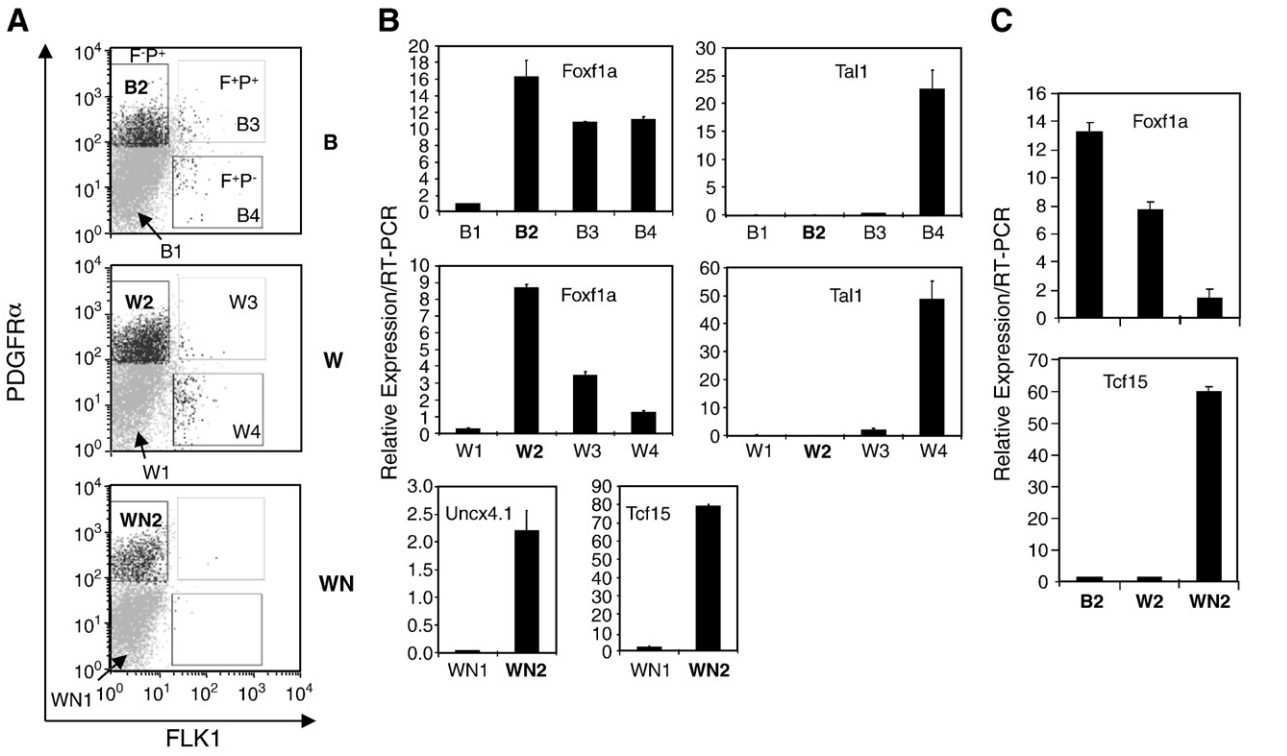

Figure 5 The $(N^+)F^-P^+$ cells commonly generated from ES cells in the presence of BMP4, WNT3a, or WNT3a + NOG in CDM express distinct sets of mesodermal genes. (A) The E14 ES cells were differentiated in CDM in the presence of BMP4 (B), 100 ng/ml WNT3a (W), and WNT3a + 0.5 μg/ml NOG (WN). EB cells were sorted on Day 5: F^-P^- (gate B1, W1, WN1); $(N^+)F^-P^+$ (gate B2, W2, WN2); F^+P^+ (gate B3, W3); F^+P^- (gate B4, W4). There were too few F^+P^+ and F^+P^- generated in the presence of WNT3a + NOG to analyze. (B) Relative expression of lateral plate/extraembryonic mesoderm and somitic mesoderm genes. Real-time RT-PCR was performed on the indicated sets of fractions with primers for Foxf1a, Tal1, Uncx4.1, and Tcf15. Data are representative of 3 independent experiments. (C) Expression of Foxf1a (a lateral plate/extraembryonic mesoderm gene) and Tcf15 (a paraxial mesoderm gene) in differently generated $(N^+)F^-P^+$ fractions. (B, C) The results are average relative expression levels with SD shown as thin vertical lines. Data are representative of 3 independent experiments.

Exogenous BMP4 induced somewhat lower levels of F^-P^+ cells than WNT3a (Fig. 4A), and a similar set of genes to WNT3a (Fig. 4B). Stimulation by either BMP4 (Fig. 4B, lane 4/B) or WNT3a (lane 6/W) induced the expression of T and Tbx6, a response similar to that of lateral plate/extraembryonic mesoderm genes. Suppression by FZD (Fig. 4B, lane 5/BF) of all signals stimulated with BMP4 supported the idea that WNT signaling is essential. However, WNT3a stimulation of T and Tbx6 gene expression was resistant to NOG (Fig. 4B, lane 7/WN), suggesting that BMP signaling is not essential. These observations are consistent with those with the use of KSR medium (Fig. 1C). Interestingly, the response to the addition of BMP4 and WNT3a together was similar to that for BMP4 alone (Fig. 4A, BW, and Fig. 4B, lane 8/BW).

Development of chondrogenic mesoderm in a chemically defined medium corresponds to somitic mesoderm specification

The F^-P^+ chondrogenic mesoderm was derived from ES cells in KSR-based serum-free medium, dependent on endogenous WNT activity (Fig. 3). Therefore, we determined whether the F^-P^+ mesoderm induced with an optimal concentration of WNT3a in CDM of 100 ng/ml was similarly chondrogenic.

ES cells were differentiated in CDM in the presence of BMP4, WNT3a, or WNT3a and NOG. Then, P^+ and/or F^+ EB cell fractions were sorted and subjected to real-time RT-PCR analysis (Fig. 5) and 2D-micromass culture (Fig. 6). In all cases, the major differentiated cell populations were F^-P^+ (Fig. 5A, B2,W2,and WN2) and the very small, minor fractions were F^+P^+ cells (B3 and W3) or F^+P^- cells (B4 and W4) cogenerated in the presence of BMP4 and WNT3a, respectively. Like the F^+ and P^+ progeny generated in the KSR medium, these cells were both N^+ and T^+, as confirmed with GFP-Bry ES cells (S. Fig. 5A), and the expression of mesoderm genes was invariably confined to the F^+ or P^+ cell fractions (Fig. 5B). For example, in the presence of WNT3a alone, cells expressing lateral plate/extraembryonic mesoderm genes such as Hand2 (data not shown) and Foxf1a were enriched in the F^-P^+ fraction (W2), although the expression was more widely distributed among F^+ and P^+ progeny generated in the presence of BMP4 (B2–B4). Similarly, ES cell progeny of the same surface phenotype (F^-P^+) but generated in the presence of WNT3a and NOG (Fig. 5A, WN2) were enriched in cells expressing somitic/rostral presomitic mesoderm genes such as Meox1 (data not shown), Tcf15, and Uncx4.1 (Fig. 5B, WN2). Among F^-P^+ cells, the level of Tcf15 mRNA was highest and that of Foxf1a mRNA was lowest in those derived from WNT3a plus NOG-treated EBs (Fig. 5C, WN2). Tal1 expression, a sign of hemoangiogenic

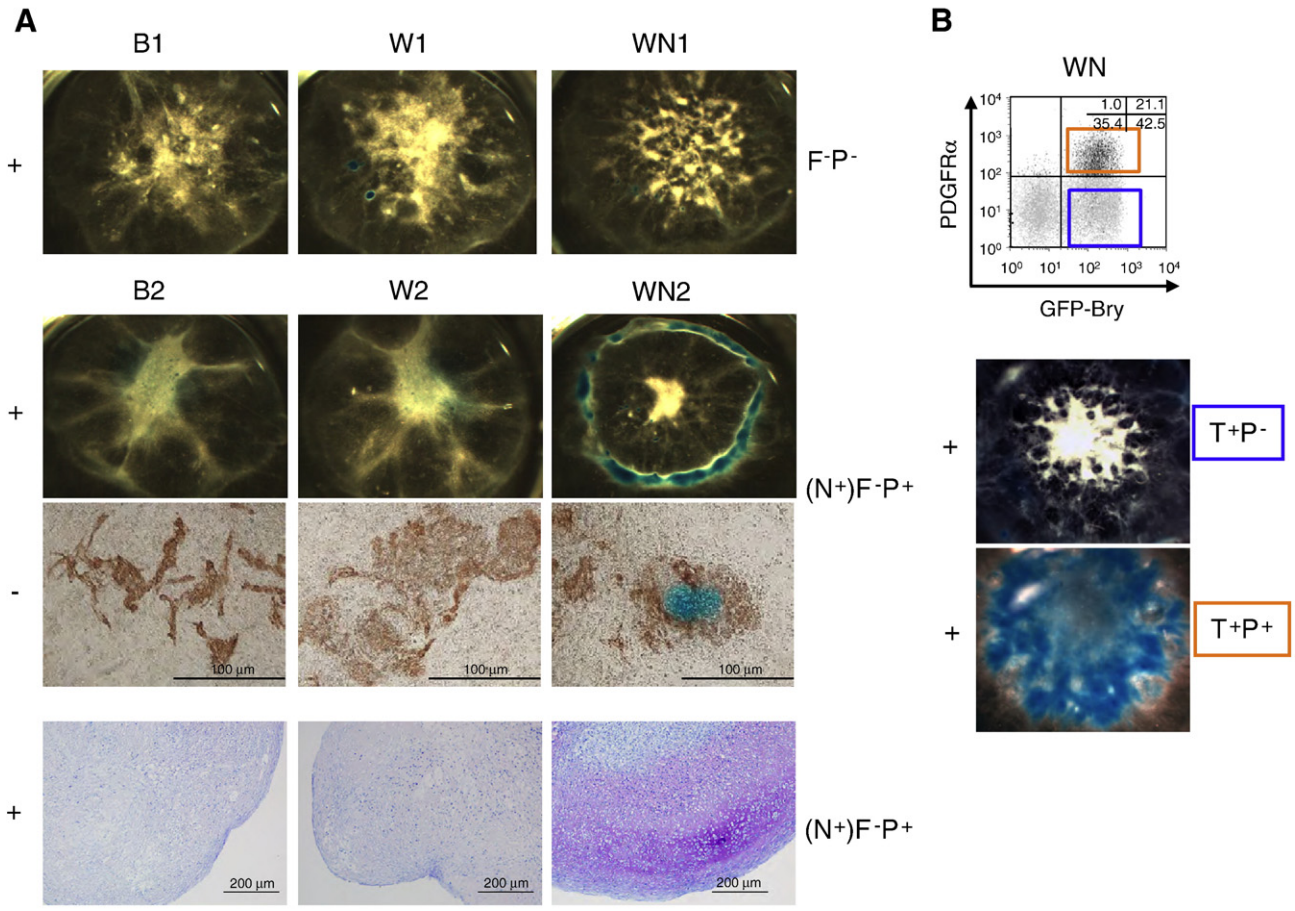

Figure 6 Chondrogenic activity is preferentially found in the F^-P^+ cell fraction generated in the presence of WNT3a and NOG. (A) The E14 ES cells were differentiated in CDM and EB cell fractions were collected by cell sorting, as in Fig. 5A. (Rows 1–3) The F^-P^- fractions (B1, W1, WN1) and $(N^+)F^-P^+$ fractions (B2, W2, WN2) were each subjected to 2D micromass culture for 12 to 14 days in 2DFP with (+) or without (–) TGFβ3. The micromass was fixed and stained with Alcian Blue to visualize cartilage nodules (dark field view panels in rows 1 and 2) or with Alcian Blue then F36.5B9 to detect cardiomyocytes (row 3). (Row 4) Some of the B2, W2, and WN2 cell-derived (+) micromass cultures were transferred to pellet culture in the presence of TGFβ3. Seven to 8 days later, pellets were Zn-formalin fixed, paraffin-embedded, sectioned, and subjected to metachromatic staining with Toluidine blue. (B) The GFP-Bry ES cells were differentiated in CDM in the presence of WNT3a and NOG (WN), and the $T(GFP)^+P^+$ fraction (orange square) and T^+P^- fraction (blue square) were collected by cell sorting (top panel). The sorted T^+P^+ and T^+P^- fractions were each subjected to 2D micromass culture for 12 to 14 days in 2DFP with (+) TGFβ3. The micromass was fixed and stained with Alcian Blue to visualize cartilage nodules (dark field view).

mesoderm formation, was confined to the F^+P^- fraction (Fig. 5B, B4 and W4). Thus, the transcript profiles in the EB cell fractions generated in either CDM or KSR medium appear to be similar (Fig. 2). [Note that F^-P^+ progeny derived from WNT3a+NOG-treated EBs are indicated with N^+ hereafter to distinguish them from progeny derived from BMP4- or WNT3a-treated EBs.]

Consistent with the gene expression profiles, none of the sorted $(N^+)F^-P^+$ (B2,W2,and WN2) cells showed hemogenic activity on OP9 cells (data not shown), although they were capable of generating spontaneously beating cardiomyocyte-like cells expressing cardiac β-myosin (Fig. 6, row 3). The F^+P^- cell fraction generated at low levels in the presence of WNT3a (Fig. 5A, W4) displayed a high degree of lymphohemogenic potential on OP9 cells (data not shown). These biological activities enriched in the F^-P^+ and F^+P^- cell fractions from CDM are thus similar to those in the corresponding progeny generated in KSR medium (Figs. 2 and 3) (Nakayama et al., 2003). However, the chondrogenic activity commonly enriched in the F^-P^+ cell fraction was differentially generated (E14 cells: Fig. 6A, rows 1, 2 and 4; EBRTcH cells: S. Fig. 5C, left 2 panels). Both 2D-micromass culture and pellet culture demonstrated that cartilage nodule-forming activity was generated from ES cells specifically with WNT3a and NOG and correlated with the accumulation of somitic mesoderm-like cells (Fig. 6A, WN2). In contrast, no appreciable chondrogenic activity was generated with WNT3a or BMP4 when lateral plate/extraembryonic mesoderm-like cells accumulated (Fig. 6A, W2 and B2). To confirm that the chondrogenic $N^+F^-P^+$ cells are mesodermal (T^+ cells), the GFP-Bry ES cells were differentiated in CDM in the presence of WNT3 and NOG (Fig. 6B). Chondrogenesis assay by 2D-micromass culture, performed using the sorted $T/GFP^+(F^-)P^+$ and $T^+(F^-)P^-$ EB cells (orange and blue squares, respectively), demonstrated that the robust chondrogenic activity was associated with the

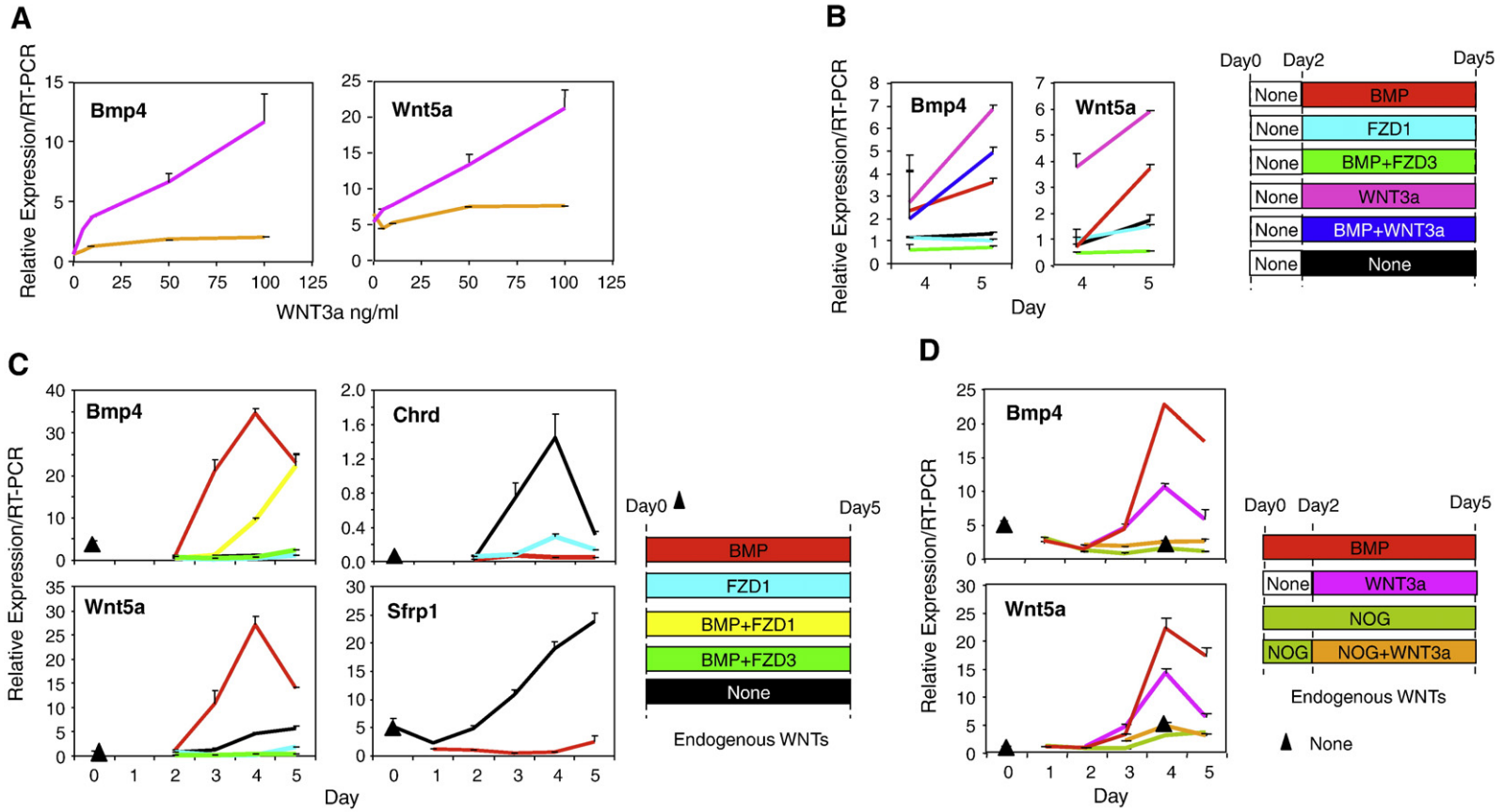

Figure 7 Exogenous WNT3a or BMP4 stimulates expression of both Bmp and Wnt genes. Gene expression was analyzed by real-time RT-PCR as in Fig. 4C using the indicated primers. (A) The E14 ES cells were differentiated in CDM in the presence (orange line) or absence (purple line) of 0.5 μg/ml NOG and various concentrations of WNT3a. (B) E14 cells were differentiated in CDM plus BMP4 (BMP), 1 μg/ml FZD (FZD1), BMP4 + 3 μg/ml FZD (BMP + FZD3), 100 ng/ml WNT3a (WNT3a), or BMP4 + WNT3a (BMP + WNT3a). Right panel: timing of factor addition (color coded). Line color corresponds to the color code. (C) E14 cells were differentiated in KSR-based serum-free medium in the presence or absence of BMP4 with 0, 1, or 3 μg/ml FZD. (D) E14 cells were differentiated in KSR-based serum-free medium in the presence or absence of WNT3a with 0.0 or 0.5 μg/ml NOG. (C, D) Right panel: timing of factor addition (color coded). The line color corresponds to the color code. ▲, No-addition control. Results are presented as average relative expression levels with SD shown as thin vertical lines and are representative of 3 independent experiments.

T^+P^+ cell fraction. Thus, during ES cell differentiation in CDM, the appearance of chondrogenic activity was strongly associated with $N^+F^-P^+$ somitic/rostral presomitic mesoderm specification, which requires WNT3a and NOG, but not with F^-P^+ lateral plate/extraembryonic mesoderm specification, which requires either WNT3a or BMP4.

Either BMP4 or WNT3a stimulates WNT and BMP signaling, potentially through enhancing endogenous production of WNT and BMP activities, respectively

As judged by in vitro developmental potential, FLK1/PDGFRα expression profiles, and gene expression profiles, lateral plate/extraembryonic mesoderm specification by either exogenous BMP4 or WNT3a during ES cell differentiation involved both WNT and BMP signaling, regardless of the type of serum-free medium used (Figs. 1, 4, and 5). Furthermore, somitic/rostral presomitic mesoderm specification was dependent on silencing of the endogenous BMP functions, especially when an optimized level of WNT3a was provided in CDM (Figs. 1, 4, and 5). One explanation for these phenomena is that exogenous BMP4 and WNT3a induce production of active WNTs and BMPs, respectively, from differentiating ES cells in either medium used. This possibility was investigated further.

During ES cell differentiation in KSR-based serum-free medium, exogenous BMP4 caused a significant upregulation of Wnt5a (Figs. 7C and D, and S. Fig. 1C, red) and Wnt4 (S. Fig. 2C, lane 5) mRNAs and a more modest upregulation of Wnt2, Wnt5b, and Wnt11 mRNAs (data not shown). In addition, BMP4 suppressed the level of transcription of the soluble Wnt inhibitor genes, Sfrp1 (Fig. 7C, red) and Sfrp2 (data not shown). Consistent with this observation, BMP4 induction of Wnt5a expression (Fig. 7B), and Wnt3 expression to a lesser degree (data not shown), was also observed during ES cell differentiation in CDM.

On the other hand, exogenous WNT3a was found to elevate expression of Bmp2, Bmp4, and other Bmp transcripts during ES cell differentiation either in KSR medium or in CDM (Fig. 7 and S. Fig. 2C). For example, the Bmp4 transcripts were induced from Days 3 to 4 of differentiation in the presence of WNT3a. WNT3a also caused an increase in the mRNA level of Wnt5a, resembling the effect of exogenous BMP4 (Figs. 7A, B, and D). The expression levels of both Bmp4 and Wnt5a genes correlated positively with the concentration of WNT3a (Fig. 7A, purple), which was counteracted by addition of NOG (orange).

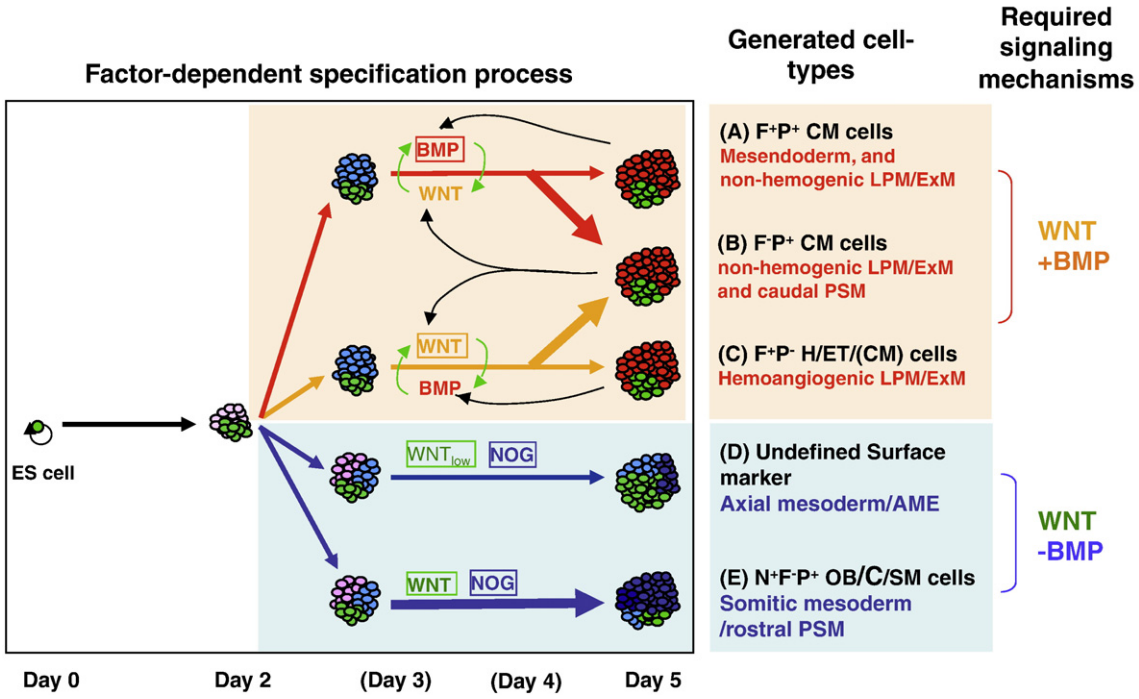

Figure 8 Differentiation of the WNT-dependent mesoderm specification process by BMP signaling. (WNT + BMP) Activation of BMP signaling (red BMP in square) or WNT signaling (orange WNT in square) from Day 2 leads to specification of lateral plate mesoderm (LPM) and/or extraembryonic mesoderm (ExM) displaying cardiomyogenic (CM, red arrows), and hemogenic mesoderm (H, orange arrows). Increased levels of Bmp and Wnt transcripts in cells already specified to LPM/ExM/H may provide active BMPs and WNTs that together facilitate the LPM/ExM specification process (black thin arrows). (WNT-BMP) Activation of WNT signaling (green WNT in square) without BMP signaling (blue NOG in square) leads to axial mesoderm and/or axial mesendoderm (AME) specification as well as somitic mesoderm and/or rostral presomitic mesoderm (PSM) specification (blue arrows). Axial mes(end)oderm specification requires less that 5% of the concentration of WNT3a (WNT_{low}) required for specification of other mesoderm. With a higher concentration of WNT3a, NOG is required to suppress coactivation of BMP signaling. Developmental potentials toward chondrocytes (C), endothelial cells (ET), osteoblasts (OB), and skeletal myocytes (SM) are also indicated.

These results support the predicted model: mutual stimulation of ligand production would be the key mechanism, leading to the phenomenon in which exogenous BMP4 or WNT3a alone induces differentiation events that depend on both BMP and WNT signaling from ES cells in either serum-free medium.

Discussion

During the first 5 days of ES cell differentiation, (1) WNT signaling under conditions of suppressed BMP signaling stimulated the generation of cells with robust osteochondrogenic and myogenic activities expressing somitic/rostral presomitic mesoderm genes (Fig. 8E, blue arrows), (2) WNT signaling together with BMP signaling stimulated the production of (cardio)myogenic cells expressing lateral plate/extraembryonic mesoderm genes (Figs. 8A–C, orange and red arrows), (3) stronger WNT signaling is required for lateral plate/extraembryonic and somitic/rostral presomitic mesoderm specification than for axial mes(end)oderm specification, and (4) there is a positive cross talk relation between Bmp and Wnt expression mechanisms during ES cell differentiation (Figs. 8A–C, black and green thin arrows), so that stimulation by either BMP or WNT initiates both signaling events.

We have previously reported that F^-P^+, F^+P^+, and F^+P^- progeny generated in the presence of BMP4 in KSR-based serum-free medium display chondrogenic activity, and that only the F^+P^- fraction shows hemogenic activity (Nakayama et al., 2003). In support of the earlier finding that BMP and WNT signaling coordinately specify hematopoietic progenitors (Lengerke et al., 2008; Nostro et al., 2008), the genesis of these progeny depended on both BMP and WNT signaling, and they expressed genes marking lateral plate/extraembryonic mesoderm, but not somitic/rostral presomitic mesoderm (Figs. 1 and 2). On the other hand, in CDM, WNT3a, or BMP4 stimulated the genesis from ES cells of F^-P^+ progeny that also expressed lateral plate/extraembryonic mesoderm genes in a similar way that depended on both WNT and BMP signaling (Figs. 4 and 5).

When BMP signaling was kept at low levels (e.g., in the absence of BMP4 in the KSR medium or in the presence of WNT3a and NOG in CDM), $N^+F^-P^+$ progeny commonly accumulated, which were enriched in cells expressing somitic/rostral presomitic mesoderm genes (Figs. 2 and 5) and exerted osteochondrogenic activity (Figs. 3 and 6), irrespective of the differentiation medium. These observations were made reproducibly with three ES cell lines examined (Fig. 6 and S. Fig. 5C). Somitic (paraxial) mesoderm is specified in the distal part of the mouse embryo, where BMP signaling is prevented by the BMP inhibitors secreted from distal visceral endoderm and axial mes(end)oderm (Bachiller et al., 2000; Loebel et al., 2003; del Barco Barrantes et al., 2003). The lack of BMP signaling through BMPR1A during gastrulation in the mouse results in ectopic somite formation and concomitant loss of lateral plate mesoderm (Miura et al., 2006). Maintenance of the somite state requires continuous BMP inhibition (Tonegawa et al., 1997; Tonegawa and Takahashi, 1998), and BMP inhibition later stimulates the expression of Pax1 and concomitant genesis of sclerotome, i.e., osteochondrogenic mesenchymal cell derived from the ventral part of somite (Dockter, 2000; Monsoro-Burq and Le Douarin, 2000). Since the $N^+F^-P^+$ chondrogenic somitic/rostral presomitic mesoderm fraction exclusively accumulates the Pax1 (S. Figs. 2A and 3A) and Pax9 transcripts (data not shown), and immunostaining of EBs with antibody to MEOX1 showed no distinct somite-like structures (data not shown), we suggest that continuous suppression of BMP-signaling during mesoderm specification by WNT signaling is sufficient to specify sclerotomal cells directly from ES cells.

In contrast, the genesis of chondrogenic activity from ES cells was strikingly inefficient (Fig. 6), and the levels of F^+P^+ and F^+P^- progeny were much lower in CDM plus WNT3a alone, BMP4 alone, or WNT3a and BMP4 (Figs. 4 and 5) than in KSR medium plus BMP4 (Figs. 1–3, and Nakayama et al., 2003). These data suggest that nonchondrogenic lateral plate mesoderm is specified preferentially in CDM when BMP and WNT signaling are activated, and/or that CDM lacks the ability to support maturation of the specified (early) lateral plate mesoderm to become chondrogenic. For example, an additional signaling mechanism essential for the genesis of (F^+) lateral mesoderm-derived chondrogenic cells may not have been activated. As in the recent reports (Nostro et al., 2008; Takenaga et al., 2007), the major candidate for the unidentified signaling could be the pathway activated by Activin, Nodal, or Nodal-related molecules. In this regard, it is worth noting that KSR contains undefined proprietary components (patent PCT/US98/00467; WO98/30679). Therefore, as it supports endogenous WNT production, KSR may also stimulate other signaling mechanisms. BMP signaling seems to impose posterior-proximal positional identity (Loebel et al., 2003; Gadue et al., 2006) and/or lateral identity (Miura et al., 2006; Tonegawa et al., 1997; Tonegawa and Takahashi, 1998) in EB cells, a possibility supported by our microarray analysis of sorted cell fractions (S. Fig. 4). Therefore, BMP's positional effects may be exaggerated in CDM, leading to a narrow spectrum of cell types to be specified by WNTs. Furthermore, lack of endoderm involvement may account for the inefficient specification of chondrogenic lateral mesoderm by WNT3a or BMP4 in CDM. In support of this suggestion, transcription of the early endoderm marker, Goosecoid (Gsc), and the primitive/definitive endoderm marker, Sox17, was induced in CDM by a low concentration of WNT3a (5 ng/ml) or by a higher concentration of WNT3a (50–100 ng/ml used for generating mesoderm) with NOG (S. Fig. 5B). BMP4 alone showed very little induction of Gsc or Sox17 (data not shown).

FACS separation of EB cells with a combination of cell surface markers such as CDH2, FLK1, and PDGFRα was useful for the simultaneous identification and isolation of different types of progeny. Microarray (S. Fig. 2 and S. Table 2) and real-time RT-PCR analyses (S. Fig. 3) have indicated that the $N^+F^-P^-$ fraction (lane 4), obtained at the same time with the $N^+F^-P^+$ somitic/rostral presomitic mesoderm (lane 3), uniquely exhibits features of neural progenitors, expressing Sox1, Pax6, and other neural transcripts. On the other hand, the $N^-F^-P^-$ cells (lane 2) were enriched in the ES cell transcripts, Pou5f1, Zfp42/Rex1, and Nanog, but the presence of the epiblast transcript, Fgf5, suggested some contamination with epiblasts. These results were reproduced with more than one ES cell line tested (S. Fig. 3).

Direct mRNA analyses have indicated that exogenous WNT3a induces BMP production, which in turn induces Wnt

expression, and that BMP4 induces WNT production that leads to Bmp expression (Fig. 7 and S. Fig. 1C). These results strongly suggest a cross talk relation between Bmp and Wnt expression mechanisms during ES cell differentiation. We have proposed two mechanisms to explain these phenomena: one based on a simple positive feed back mechanism (Fig. 8, thin black arrows), and the second assuming transcriptional cross talk between Wnts and Bmps, in that WNTs induce Bmp expression and vise versa (thin green arrow). The first model depends on differentiation, which is initiated by either exogenous WNTs or BMPs, and the supply of both WNTs and BMPs by differentiated progeny. In support, transcripts of various Bmp and Wnt genes (Bmps 2, 4, 5 and 6, and Wnts 4 and 5a) were preferentially detected in the differentiated progeny (F^+ and P^+ cells, S. Fig. 2C). Therefore, BMP and WNT production levels would correlate with the degree of differentiation. The second model implies that at a certain stage of differentiation, stimulation by either WNTs or BMPs leads to the cycle of reciprocal stimulation of WNT and BMP production independent of, or parallel with, the differentiation.

Functional interactions between TGFβ and Wnt signaling (von Bubnoff and Cho, 2001) and between BMP and Wnt signaling (Szeto and Kimelman, 2004) have been demonstrated during early zebrafish embryogenesis. Positive cross talk between BMP2/4 and Xwnt8 during ventrolateral mesoderm specification is also shown in Xenopus (Hoppler and Moon, 1998; Marom et al., 1999). Recently, a positive Wnt–BMP interaction has been demonstrated during primitive streak formation from human ES cells (Sumi et al., 2008). Our results suggest that a similar mechanism may be present during lateral plate and extraembryonic mesoderm specification in the mouse.

The process of WNT-induced mesoderm specification does not always involve BMP signaling. For example, BMP-sensitive somitic/rostral presomitic mesoderm specification was induced by endogenous WNTs in KSR medium in the absence of NOG (Fig. 1). It is unclear what determines the production of BMPs and involvement of BMP signaling during the WNT-induced differentiation events. They may depend on the strength of WNT signaling. Given that the WNT3a-induced mesendoderm specification occurred in the absence of NOG only at low concentrations of WNT3a (Fig. 4C), the BMP-independent WNT effects may be realized when WNT signaling is weak. However, this model cannot explain the NOG-independent specification of somitic/rostral presomitic mesoderm by WNT in KSR medium (Figs. 1 and 2), since the process is expected to require stronger WNT signaling (Fig. 4C). In contrast, the endogenous Wnt transcripts that accumulated spontaneously under this condition were Wnt7a and Wnt8a and were not the same as those induced in the presence of BMP4 (Fig. 7, and S. Figs. 1B and 2C). Therefore, the reason may be that different WNT proteins are induced, which in turn induce different progeny expressing different levels and types of BMPs.

Thus, comparison of the effects of different factor-dependent differentiation culture methods has led to a better understanding of how the processes of specification of particular mesoderm and generation of specific biological activities during ES cell differentiation are regulated by extracellular factors. One of the most important outcomes of this comparative study is the notion that the response of differentiating ES cells to exogenous factors can be context (e.g., medium) dependent. This consideration is especially important in relation to the generation from human ES cells or iPS cells of clinically relevant chondrogenic cells in chemically defined/serum-free media.

Materials and methods

Cells, factors, and antibodies

Mouse E14 ES cells were obtained and cultured as described previously (Nakayama et al., 1998, 2003). GFP-Bry ES cells and Rosa26 ES cells were provided by G. Keller (Toronto, Canada) and P. Soriano (Seattle, WA), respectively, and both were cultured as for the E14 ES cells. EBRTcH3 ES cells were provided by H. Niwa (Kobe, Japan) and were maintained as described (Masui et al., 2005). Antibodies for FACS, cytokines, media and supplements, buffers and specialized tissue culture plates were generally sourced as described (Nakayama et al., 1998, 2000, 2003). Biotin-conjugated anti-PDGFRα antibody was from eBioscience (San Diego CA), and phycoerythrin (PE)-Cy7-conjugated streptavidin was from BD Bioscience (North Ryde, Australia).

Anti-CDH2 antibody was from Santa Cruz Biotech (Santa Cruz, CA), allophycocyanin (APC)-conjugated secondary antibody was from Molecular Probes/Invitrogen (Eugene, OR), mouse anti-skeletal myosin sarcomere monoclonal antibody (clone MF20) was from Developmental Studies Hybridoma Bank (University of Iowa, Iowa), mouse anti-ventricular β-myosin monoclonal antibody (clone F36.5B9) was from AXXORA (Sapphire Bioscience, Crows Nest, Australia), and mouse DKK1 and FZD were from R&D. Mouse Wnt3a protein was prepared according to the published procedure (Willert et al., 2003; Davidson et al., 2007).

Differentiation induction by the embryoid body formation method

ES cells were precultured without feeder for 24 h on a fibronectin-coated plate (BD) in the KSR-based serum-free preculture medium: Iscove modified Dulbecco medium (IMDM, Sigma-Aldrich, Sydney, Australia), 15% (v/v) KSR (Invitrogen, Thornton, Australia), 2 mM GlutaMax (Invitrogen), 0.15 mM monothioglycerol (MTG, Sigma), supplemented with 1000 U/ml ESGRO (10 ng/ml leukemia inhibitory factor, Chemicon, Boronia, Australia (Nakayama et al., 2003, 2000). EBs were then formed from either 5×10^3 single ES cells/ml in KSR-based serum-free differentiation medium (KSR medium) (Nakayama et al., 2000, 2003) or 1.2×10^4 single ES cells/ml in CDM (Johansson and Wiles, 1995; Wiles and Johansson, 1999). The KSR-medium consisted of IMDM 15% (v/v) KSR, 2 mM GlutaMax, 100 μg/ml bovine holotransferrin (Sigma), 10 μg/ml bovine insulin (Invitrogen), 0.45 mM MTG, and 0.9% (w/v) methylcellulose (Stem Cell Technology, Vancouver, Canada). CDM was composed of IMDM:Ham's F12 (1:1), 5 mg/ml fatty acid-free bovine serum albumin (Sigma), 2% (v/v) chemically defined lipid concentrate (Invitrogen), 2 mM GlutaMax, 100 μg/ml holotransferrin, 10 μg/ml insulin, 0.45 mM MTG, 10 U/ml ESGRO (0.1 ng/ml leukemia inhibitory factor, Chemicon, Boronia, Australia), and 0.9% (w/v) methylcellulose.

Analytical scale was 3–5 ml and preparative scale was 64 ml. As specified, the medium was supplemented, usually on Day 2 of differentiation, with NOG, DKK1 and/or FZD at 0.05–3 μg/ml, WNT3a at 5–250 ng/ml, and BMP4 at 2 ng/ml (Nakayama et al., 2000).

Flow cytometry on embryoid body cells

Immunostaining of EB cells for flow cytometry was as described (Nakayama et al., 2003) with the following modifications: anti-CDH2 antibody visualized by AlexaFluoro488 (Molecular Probes, Eugene, OR) or allophycocyanin (BD) was incorporated as indicated for fractionating EB cells; FACS analysis was performed on LSRII (BD) or FC500 (Beckman-Coulter, Gladesville, Australia); cell sorting was done with DIVA (BD) or Influx (Cytopia-BD) using the 4-way cell-sorting capability, and viable single cells were gated using Fluoro-Gold (Invitrogen-Molecular Probes) or propidium iodide (Sigma). Sorted cells ranged in purity from 91 to 97%.

Chondrogenesis and myogenesis assays

Pellet- and 2D-micromass cultures for the primary chondrogenesis assays were as described (Nakayama et al., 2003) with minor changes; the 2D-micromass medium was supplemented either with 1% (v/v) fetal bovine serum (FCS, Hyclone, Logan UT) and 40 ng/ml PDGF-BB (2DFP) or with 2% (v/v) FCS (2DFCS). TGFβ3 (R&D) was added at 10 ng/ml, and cultures were maintained for 12–14 days. For histological confirmation of chondrocyte formation, the cell mass was scraped on Day 10 and transferred to a tube for pellet-micromass culture for 7–8 days. A 2D-micromass culture without TGFβ3 was used for the myogenesis assay.

The 2D-micromass cultures were washed once, fixed with 10% (v/v) buffered Zn-formalin (Shandon/Thermo, Waltham MA), and stained first with 1% (w/v) Alcian Blue pH 1.0 (Nakayama et al., 2003). Cells were then immunostained with MF20 or F36.5B9 and color developed with metal-enhanced DAB (Pierce, Rockford, IL) or Fast Red TR/AS-MX (Pierce). The pellet culture was fixed with Zn-formalin, paraffin-embedded, sectioned, and stained with 0.1% (w/v) Toluidine blue (Nakayama et al., 2003).

Transient expansion of FACS-purified EB cells, and osteogenic assay

FACS-purified EB cells were plated at $1.0–2.5\times10^4$ cells/well in a 24-well, fibronectin-coated plate and maintained in the original serum-free 2D-medium (Nakayama et al., 2003) with 50–100 ng/ml human insulin-like growth factor and 12.5–25 ng/ml human fibroblast growth factor (2DIF) at 37 °C in 5% O_2, 10% CO_2. Osteogenesis was induced at 70–80% confluence by changing the medium to BOM: α-modified minimal essential medium (αMEM, GIBCO), 10% (v/v) FCS, 0.1 μM dexamethasone, 0.1 mM ascorbic acid-2-phosphate, 10 mM β-glycerophosphate (all from Sigma). One well for the un-induced control was maintained in SCGM: αMEM, 10% (v/v) FCS. Three to 4 weeks later, wells were washed three times with 10 mM Tris-HCl (pH 7–8), fixed with 10% (v/v) neutral-buffered formalin, and stained with 2% (w/v) Alizarin red (Sigma).

Gene-expression profiling of EB cells

Real-time PCR

Total RNAs from whole EBs and FACS-purified EB cells were purified with QIA Shredder and RNeasy Micro Kit (Qiagen, Doncaster, Australia). Reverse transcription (Nakayama et al., 1998) was followed by real-time PCR using SYBR Green PCR Master Mix or the Taqman system (Applied Biosystems, Foster City CA) and analysis with ABI7500 (Applied Biosystems). For the SYBR Green method, the primers (S. Table 1) were synthesized by Geneworks (Thebarton, Australia). Individual gene expression levels from duplicate or triplicate reactions were normalized against Eef1a1 transcript and averaged to obtain relative expression (relative expression/RT-PCR).

Microarray analysis

The EB cells in KSR-based serum-free medium were sorted for PDGFRα and FLK1 expression in the case of BMP4-treated cultures (total of four fractions), or for PDGFRα and CDH2 expression for the BMP4-untreated culture (total of three fractions). Total RNA was prepared from 10^4 cells from each of seven FACS-purified cell fractions plus two unsorted cell controls for BMP4-treated and -untreated EBs. RNA preparations were linearly amplified twice by Two-Cycle Target Labeling and Control Reagents (Affymetrix, Santa Clara CA), and hybridized to the Mouse Genome 430–2.0 Array (Affymetrix). Experiments were repeated three times. Affymetrix CEL files of all samples were background-corrected, normalized, and analyzed using default parameters of the GC-RMA method (Wu and Irizarry, 2004) to obtain the relative expression value (relative expression/microarray) of each gene. Data were analyzed using GeneSpring software (Agilent Technologies, Palo Alto CA). Genes that gave consistent expression levels over the three experiments ($P<0.05$) were included in fraction-specific gene lists (S. Table 2).

Acknowledgments

We acknowledge M. Vanevski, B. Wang, and S. Li for technical assistance with cell culture and real-time RT-PCR analysis, and R. Driessen for microarray data acquisition. We also warmly thank R. Rossi and A. Fryga for cell sorting, J. Javni for administrative assistance, and P. Tam for critical reading of earlier versions of this manuscript. This work was supported by the Adult Stem Cell Platform Fund (P015, P.S.) and the Haemopoiesis Therapeutic Focus Fund (P017, P.S./N.N., and P009, N.N.) from the Australian Stem Cell Centre.

Appendix A. Supplementary data

Supplementary data associated with this article (S. Figs and S. Tables) can be found, in the online version, at doi:10.1016/j.scr.2009.07.001.

References

Ang, S.L., Wierda, A., Wong, D., Stevens, K.A., Cascio, S., Rossant, J., Zaret, K.S., 1993. The formation and maintenance of the definitive endoderm lineage in the mouse: involvement of HNF3/forkhead proteins. Development 119, 1301–1315.

Arnold, S.J., Stappert, J., Bauer, A., Kispert, A., Herrmann, B.G.,

Kemler, R., 2000. Brachyury is a target gene of the Wnt/beta-catenin signaling pathway. Mech. Dev. 91, 249–258.
Bachiller, D., Klingensmith, J., Kemp, C., Belo, J.A., Anderson, R.M., May, S.R., McMahon, J.A., McMahon, A.P., Harland, R.M., Rossant, J., et al., 2000. The organizer factors Chordin and Noggin are required for mouse forebrain development. Nature 403, 658–661.
Betsholtz, C., Karlsson, L., Lindahl, P., 2001. Developmental roles of platelet-derived growth factors. Bioessays 23, 494–507.
Breier, G., Breviario, F., Caveda, L., Berthier, R., Schnuerch, H., Gotsch, U., Vestweber, D., Risau, W., Dejana, E., 1996. Molecular cloning and expression of murine vascular endothelial-cadherin in early stage development of cardiovascular system. Blood 87, 630–641.
Burgess, R., Cserjesi, P., Ligon, K.L., Olson, E.N., 1995. Paraxis: a basic helix-loop-helix protein expressed in paraxial mesoderm and developing somites. Dev. Biol. 168, 296–306.
Burgess, R., Rawls, A., Brown, D., Bradley, A., Olson, E.N., 1996. Requirement of the paraxis gene for somite formation and musculoskeletal patterning. Nature 384, 570–573.
Candia, A.F., Hu, J., Crosby, J., Lalley, P.A., Noden, D., Nadeau, J.H., Wright, C.V., 1992. Mox-1 and Mox-2 define a novel homeobox gene subfamily and are differentially expressed during early mesodermal patterning in mouse embryos. Development 116, 1123–1136.
Chapman, D.L., Papaioannou, V.E., 1998. Three neural tubes in mouse embryos with mutations in the T-box gene Tbx6. Nature 391, 695–697.
Chapman, D.L., Agulnik, I., Hancock, S., Silver, L.M., Papaioannou, V.E., 1996. Tbx6, a mouse T-Box gene implicated in paraxial mesoderm formation at gastrulation. Dev. Biol. 180, 534–542.
Chung, Y.S., Zhang, W.J., Arentson, E., Kingsley, P.D., Palis, J., Choi, K., 2002. Lineage analysis of the hemangioblast as defined by FLK1 and SCL expression. Development 129, 5511–5520.
Darabi, R., Gehlbach, K., Bachoo, R.M., Kamath, S., Osawa, M., Kamm, K.E., Kyba, M., Perlingeiro, R.C., 2008. Functional skeletal muscle regeneration from differentiating embryonic stem cells. Nat. Med. 14, 134–143.
Davidson, K.C., Jamshidi, P., Daly, R., Hearn, M.T., Pera, M.F., Dottori, M., 2007. Wnt3a regulates survival, expansion, and maintenance of neural progenitors derived from human embryonic stem cells. Mol. Cell. Neurosci. 36, 408–415.
del Barco Barrantes, I., Davidson, G., Grone, H.J., Westphal, H., Niehrs, C., 2003. Dkk1 and noggin cooperate in mammalian head induction. Genes Dev. 17, 2239–2244.
Deutsch, U., Dressler, G.R., Gruss, P., 1988. Pax 1, a member of a paired box homologous murine gene family, is expressed in segmented structures during development. Cell 53, 617–625.
Dockter, J.L., 2000. Sclerotome induction and differentiation. Curr. Top. Dev. Biol. 48, 77–127.
Doetschman, T.C., Eistetter, H., Katz, M., Schmidt, W., Kemler, R., 1985. The in vitro development of blastocyst-derived embryonic stem cell lines: formation of visceral yolk sac, blood islands and myocardium. J. Embryol. Exp. Morphol. 87, 27–45.
Elefanty, A.G., Begley, C.G., Hartley, L., Papaevangeliou, B., Robb, L., 1999. SCL expression in the mouse embryo detected with a targeted lacZ reporter gene demonstrates its localization to hematopoietic, vascular, and neural tissues. Blood 94, 3754–3763.
Fehling, H.J., Lacaud, G., Kubo, A., Kennedy, M., Robertson, S., Keller, G., Kouskoff, V., 2003. Tracking mesoderm induction and its specification to the hemangioblast during embryonic stem cell differentiation. Development 130, 4217–4227.
Gadue, P., Huber, T.L., Paddison, P.J., Keller, G.M., 2006. Wnt and TGF-beta signaling are required for the induction of an in vitro model of primitive streak formation using embryonic stem cells. Proc. Natl. Acad. Sci. USA 103, 16806–16811.
Honda, M., Kurisaki, A., Ohnuma, K., Okochi, H., Hamazaki, T.S., Asashima, M., 2006. N-cadherin is a useful marker for the progenitor of cardiomyocytes differentiated from mouse ES cells in serum-free condition. Biochem. Biophys. Res. Commun. 351, 877–882.
Hoppler, S., Moon, R.T., 1998. BMP-2/-4 and Wnt-8 cooperatively pattern the Xenopus mesoderm. Mech. Dev. 71, 119–129.
Houston, D., Wylie, C., 2004. The role of Wnts in gastrulation. In: Stern, C. (Ed.), Gastrulation: from Cells to Embryo. Cold Spring Harbor Laboratory Press, Cold Spring Harbor, NY, pp. 521–538.
Johansson, B.M., Wiles, M.V., 1995. Evidence for involvement of activin A and bone morphogenetic protein 4 in mammalian mesoderm and hematopoietic development. Mol. Cell. Biol. 15, 141–151.
Keller, G., 2005. Embryonic stem cell differentiation: emergence of a new era in biology and medicine. Genes Dev. 19, 1129–1155.
Kraus, F., Haenig, B., Kispert, A., 2001. Cloning and expression analysis of the mouse T-box gene Tbx18. Mech. Dev. 100, 83–86.
Lako, M., Lindsay, S., Lincoln, J., Cairns, P.M., Armstrong, L., Hole, N., 2001. Characterisation of Wnt gene expression during the differentiation of murine embryonic stem cells in vitro: role of Wnt3 in enhancing haematopoietic differentiation. Mech. Dev. 103, 49–59.
Lengerke, C., Schmitt, S., Bowman, T.V., Jang, I.H., Maouche-Chretien, L., McKinney-Freeman, S., Davidson, A.J., Hammerschmidt, M., Rentzsch, F., Green, J.B., 2008. BMP and Wnt specify hematopoietic fate by activation of the Cdx-Hox pathway. Cell Stem Cell 2, 72–82.
Lindsley, R.C., Gill, J.G., Kyba, M., Murphy, T.L., Murphy, K.M., 2006. Canonical Wnt signaling is required for development of embryonic stem cell-derived mesoderm. Development 133, 3787–3796.
Liu, P., Wakamiya, M., Shea, M.J., Albrecht, U., Behringer, R.R., Bradley, A., 1999. Requirement for Wnt3 in vertebrate axis formation. Nat. Genet. 22, 361–365.
Loebel, D.A., Watson, C.M., De Young, R.A., Tam, P.P., 2003. Lineage choice and differentiation in mouse embryos and embryonic stem cells. Dev. Biol. 264, 1–14.
Mahlapuu, M., Ormestad, M., Enerback, S., Carlsson, P., 2001. The forkhead transcription factor Foxf1 is required for differentiation of extra-embryonic and lateral plate mesoderm. Development 128, 155–166.
Mankoo, B.S., Skuntz, S., Harrigan, I., Grigorieva, E., Candia, A., Wright, C.V., Arnheiter, H., Pachnis, V., 2003. The concerted action of Meox homeobox genes is required upstream of genetic pathways essential for the formation, patterning and differentiation of somites. Development 130, 4655–4664.
Mansouri, A., Yokota, Y., Wehr, R., Copeland, N.G., Jenkins, N.A., Gruss, P., 1997. Paired-related murine homeobox gene expressed in the developing sclerotome, kidney, and nervous system. Dev. Dyn. 210, 53–65.
Marom, K., Fainsod, A., Steinbeisser, H., 1999. Patterning of the mesoderm involves several threshold responses to BMP-4 and Xwnt-8. Mech. Dev. 87, 33–44.
Masui, S., Shimosato, D., Toyooka, Y., Yagi, R., Takahashi, K., Niwa, H., 2005. An efficient system to establish multiple embryonic stem cell lines carrying an inducible expression unit. Nucleic Acids Res 33, e43.
Mishina, Y., Suzuki, A., Ueno, N., Behringer, R.R., 1995. Bmpr encodes a type I bone morphogenetic protein receptor that is essential for gastrulation during mouse embryogenesis. Genes Dev. 9, 3027–3037.
Miura, S., Davis, S., Klingensmith, J., Mishina, Y., 2006. BMP signaling in the epiblast is required for proper recruitment of the prospective paraxial mesoderm and development of the somites. Development 133, 3767–3775.
Monaghan, A.P., Kaestner, K.H., Grau, E., Schutz, G., 1993. Postimplantation expression patterns indicate a role for the mouse forkhead/HNF-3 alpha, beta and gamma genes in determination of the definitive endoderm, chordamesoderm and neuroectoderm. Development 119, 567–578.

Monsoro-Burq, A.-H., Le Douarin, N., 2000. Duality of molecular signaling involved in vertebral chondrogenesis. Curr. Top. Dev. Biol. 48, 43–75.

Nakayama, N., Fang, I., Elliott, G., 1998. Natural killer and B-lymphoid potential in CD34+ cells derived from embryonic stem cells differentiated in the presence of vascular endothelial growth factor. Blood 91, 2283–2295.

Nakayama, N., Lee, J., Chiu, L., 2000. Vascular endothelial growth factor synergistically enhances bone morphogenetic protein-4-dependent lymphohematopoietic cell generation from embryonic stem cells in vitro. Blood 95, 2275–2283.

Nakayama, N., Duryea, D., Manoukian, R., Chow, G., Han, C.Y., 2003. Macroscopic cartilage formation with embryonic stem-cell-derived mesodermal progenitor cells. J. Cell Sci. 116, 2015–2028.

Neidhardt, L., Kispert, A., Herrmann, B., 1997. A mouse gene of the paired-related homeobox class expressed in the caudal somite compartment and in the developing vertebral column, kidney and nervous system. Dev. Genes Evol. 207, 330–339.

Nishikawa, S.I., Nishikawa, S., Hirashima, M., Matsuyoshi, N., Kodama, H., 1998a. Progressive lineage analysis by cell sorting and culture identifies FLK1+VE-cadherin+ cells at a diverging point of endothelial and hemopoietic lineages. Development 125, 1747–1757.

Nishikawa, S.-I., Nishikawa, S., Kawamoto, H., Yoshida, H., Kizumoto, M., Kataoka, H., Katsura, Y., 1998b. In vitro generation of lymphohematopoietic cells from endothelial cells purified from murine embryos. Immunity 8, 761–769.

Nishikawa, S.-I., Jakt, L.M., Era, T., 2007. Embryonic stem-cell culture as a tool for developmental cell biology. Nat. Rev. Mol. Cell. Biol. 8, 502–507.

Nostro, M.C., Cheng, X., Keller, G.M., Gadue, P., 2008. Wnt, activin, and BMP signaling regulate distinct stages in the developmental pathway from embryonic stem cells to blood. Cell Stem Cell 2, 60–71.

Peterson, R.S., Lim, L., Ye, H., Zhou, H., Overdier, D.G., Costa, R.H., 1997. The winged helix transcriptional activator HFH-8 is expressed in the mesoderm of the primitive streak stage of mouse embryos and its cellular derivatives. Mech. Dev. 69, 53–69.

Radice, G.L., Rayburn, H., Matsunami, H., Knudsen, K.A., Takeichi, M., Hynes, R.O., 1997. Developmental defects in mouse embryos lacking N-cadherin. Dev. Biol. 181, 64–78.

Rashbass, P., Cooke, L.A., Herrmann, B.G., Beddington, R.S., 1991. A cell autonomous function of Brachyury in T/T embryonic stem cell chimaeras. Nature 353, 348–351.

Robertson, E.J., 1987. Embryo-derived stem cell lines. In: Robertson, E.J. (Ed.), Teratocarcinomas and Embryonic Stem Cells: A Practical Approach. IRS Press, Oxford, UK, pp. 71–112.

Saga, Y., Hata, N., Kobayashi, S., Magnuson, T., Seldin, M.F., Taketo, M.M., 1996. MesP1: a novel basic helix-loop-helix protein expressed in the nascent mesodermal cells during mouse gastrulation. Development 122, 2769–2778.

Saga, Y., Hata, N., Koseki, H., Taketo, M.M., 1997. Mesp2: a novel mouse gene expressed in the presegmented mesoderm and essential for segmentation initiation. Genes Dev. 11, 1827–1839.

Sakurai, H., Era, T., Jakt, L.M., Okada, M., Nakai, S., Nishikawa, S., Nishikawa, S., 2006. In vitro modeling of paraxial and lateral mesoderm differentiation reveals early reversibility. Stem Cells 24, 575–586.

Sakurai, H., Okawa, Y., Inami, Y., Nishio, N., Isobe, K., 2008. Paraxial mesodermal progenitors derived from mouse embryonic stem cells contribute to muscle regeneration via differentiation into muscle satellite cells. Stem Cells 26, 1865–1873.

Sasaki, H., Hogan, B.L., 1993. Differential expression of multiple fork head related genes during gastrulation and axial pattern formation in the mouse embryo. Development 118, 47–59.

Srivastava, D., Thomas, T., Lin, Q., Kirby, M.L., Brown, D., Olson, E.N., 1997. Regulation of cardiac mesodermal and neural crest development by the bHLH transcription factor, dHAND. Nat. Genet. 16, 154–160.

Sumi, T., Tsuneyoshi, N., Nakatsuji, N., Suemori, H., 2008. Defining early lineage specification of human embryonic stem cells by the orchestrated balance of canonical Wnt/{beta}-catenin, Activin/Nodal and BMP signaling. Development 135, 2969–2979.

Szeto, D.P., Kimelman, D., 2004. Combinatorial gene regulation by Bmp and Wnt in zebrafish posterior mesoderm formation. Development 131, 3751–3760.

Takada, S., Stark, K.L., Shea, M.J., Vassileva, G., McMahon, J.A., McMahon, A.P., 1994. Wnt-3a regulates somite and tailbud formation in the mouse embryo. Genes Dev. 8, 174–189.

Takakura, N., Yoshida, H., Ogura, Y., Kataoka, H., Nishikawa, S., Nishikawa, S., 1997. PDGFR alpha expression during mouse embryogenesis: immunolocalization analyzed by whole-mount immunohistostaining using the monoclonal anti-mouse PDGFR alpha antibody APA5. J. Histochem. Cytochem. 45, 883–893.

Takenaga, M., Fukumoto, M., Hori, Y., 2007. Regulated Nodal signaling promotes differentiation of the definitive endoderm and mesoderm from ES cells. J. Cell Sci. 120, 2078–2090.

Tonegawa, A., Takahashi, Y., 1998. Somitogenesis controlled by Noggin. Dev. Biol. 202, 172–182.

Tonegawa, A., Funayama, N., Ueno, N., Takahashi, Y., 1997. Mesodermal subdivision along the mediolateral axis in chicken controlled by different concentrations of BMP-4. Development 124, 1975–1984.

von Bubnoff, A., Cho, K.W., 2001. Intracellular BMP signaling regulation in vertebrates: pathway or network? Dev. Biol. 239, 1–14.

Wiles, M.V., Johansson, B.M., 1999. Embryonic stem cell development in a chemically defined medium. Exp. Cell Res. 247, 241–248.

Wilkinson, D.G., Bhatt, S., Herrmann, B.G., 1990. Expression pattern of the mouse T gene and its role in mesoderm formation. Nature 343, 657–659.

Willert, K., Brown, J.D., Danenberg, E., Duncan, A.W., Weissman, I.L., Reya, T., Yates 3rd, J.R., Nusse, R., 2003. Wnt proteins are lipid-modified and can act as stem cell growth factors. Nature 423, 448–452.

Winnier, G., Blessing, M., Labosky, P.A., Hogan, B.L., 1995. Bone morphogenetic protein-4 is required for mesoderm formation and patterning in the mouse. Genes Dev. 9, 2105–2116.

Wood, H.B., May, G., Healy, L., Enver, T., Morriss-Kay, G.M., 1997. CD34 expression patterns during early mouse development are related to modes of blood vessel formation and reveal additional sites of hematopoiesis. Blood 90, 2300–2311.

Wu, Z., Irizarry, R.A., 2004. Preprocessing of oligonucleotide array data. Nat. Biotechnol. 22, 656–658 author reply 658.

Yamaguchi, T.P., Takada, S., Yoshikawa, Y., Wu, N., McMahon, A.P., 1999. T (Brachyury) is a direct target of Wnt3a during paraxial mesoderm specification. Genes Dev. 13, 3185–3190.

Yoshikawa, Y., Fujimori, T., McMahon, A.P., Takada, S., 1997. Evidence that absence of Wnt-3a signaling promotes neuralization instead of paraxial mesoderm development in the mouse. Dev. Biol. 183, 234–242.

Young, P.E., Baumhueter, S., Lasky, L.A., 1995. The sialomucin CD34 is expressed on hematopoietic cells and blood vessels during murine development. Blood 85, 96–105.